Supplementary Data

Differential Sequence Charge-clustering and Mixing-ratio Affect Stability and Dynamics of Heterotypic Peptide Condensates

Milan Kumar Hazra*

Department of Chemistry

Indian Institute of Technology, Jodhpur

NH 62, Surpura Bypass Rd, Karwar, Jheepasani, Rajasthan

INDIA, 342030

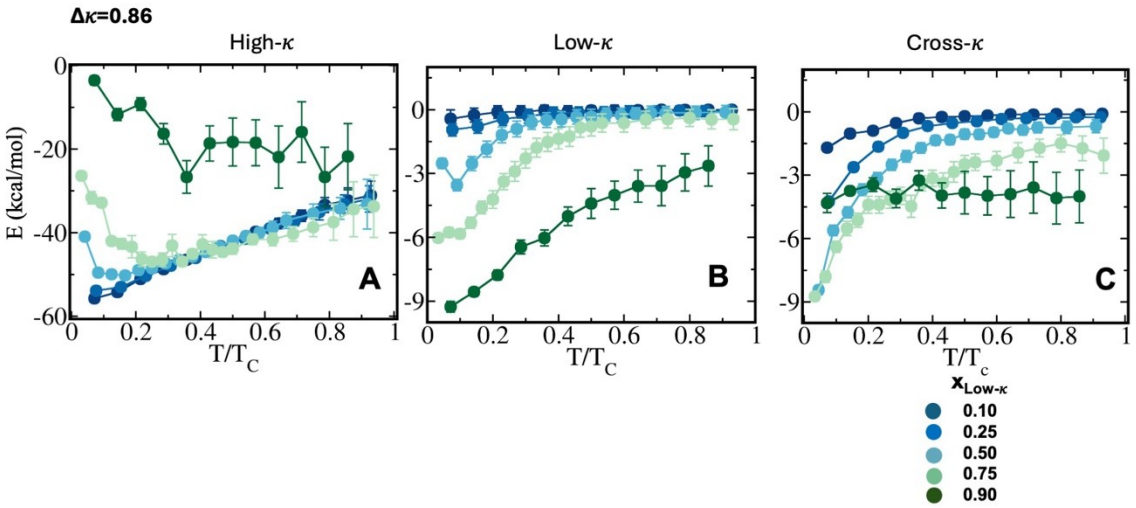

Figure S1: Dissection of total energy in self- and cross- interaction energy components in heterotypic protein condensates of sequence pairs κ=1.0 and 0.14**.** (A) Electrostatic energy among high-κ peptides that each polymer faces in condensate phase (B) Average electrostatic energy among Low-κ peptides that each polymer faces in condensate phase (C) Average electrostatic cross interaction energy among low and high-κ peptides that each polymer faces in condensate phase for sequence pairs with differential charge clustering Δκ=0.86 (sequence κ=1.0 and 0.14). Different mixing fractions has been shown in each panel ranging from $x_{Low-\kappa}$=0.1 to 0.9 with blue to green.

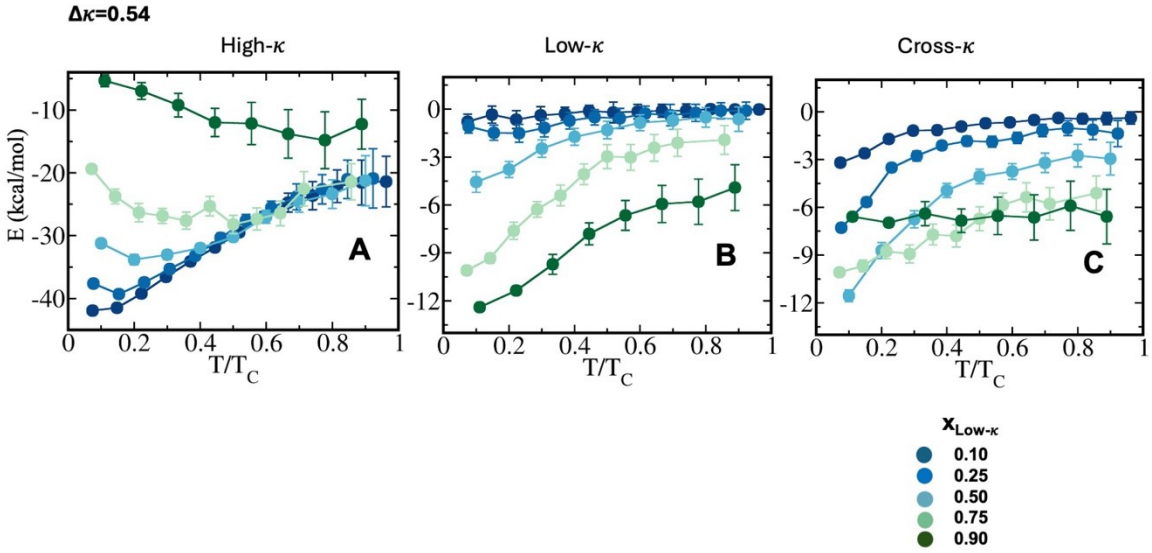

Figure S2: Dissection of total energy in self- and cross- interaction energy components in heterotypic protein condensate of sequence pairs κ=0.77 and 0.23**.** (A) Electrostatic energy among high-κ peptides that each polymer faces in condensate phase (B) Average electrostatic energy among Low-κ peptides that each polymer faces in condensate phase (C) Average electrostatic cross interaction energy among low and high-κ peptides that each polymer faces

in condensate phase for sequence pairs with differential charge clustering Δκ=0.54 (sequence κ=0.77 and 0.23). Different mixing fractions has been shown in each panel ranging from $x_{Low-\kappa}$=0.1 to 0.9 with blue to green.

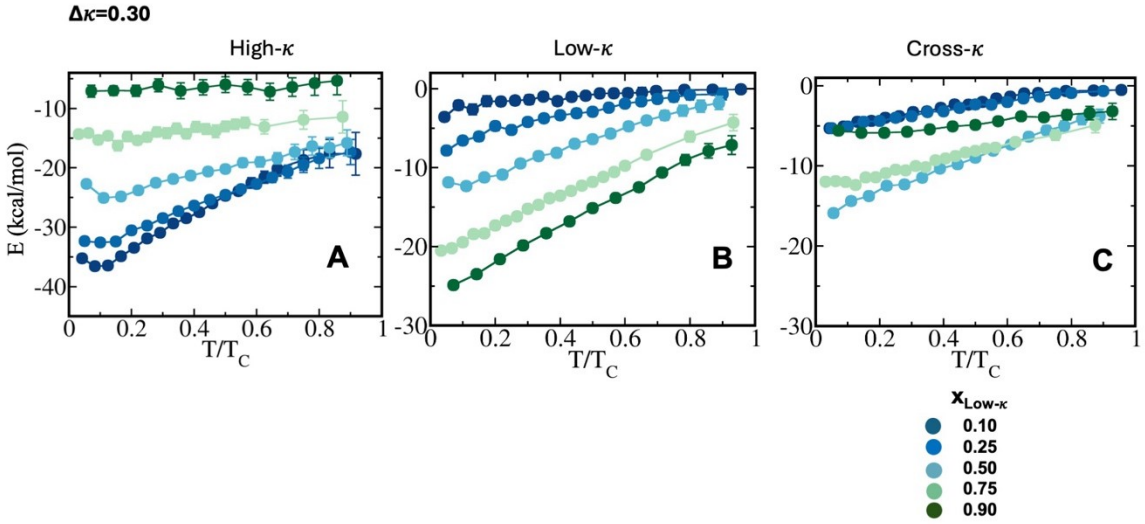

Figure S3: Dissection of total energy in self- and cross- interaction energy components in heterotypic protein condensate of sequence pairs κ=0.65 and 0.35**.** (A) Electrostatic energy among high-κ peptides that each polymer faces in condensate phase (B) Average electrostatic energy among Low-κ peptides that each polymer faces in condensate phase (C) Average electrostatic cross interaction energy among low and high-κ peptides that each polymer faces in condensate phase for sequence pairs with differential charge clustering Δκ=0.54 (sequence κ=0.65 and 0.35). Different mixing fractions has been shown in each panel ranging from $x_{Low-\kappa}$=0.1 to 0.9 with blue to green.

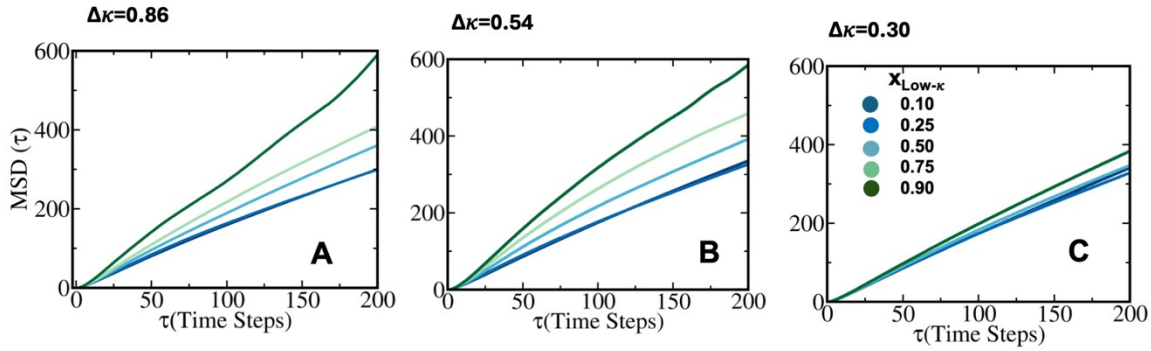

Figure S4: Average mean squared displacement (MSD) of polymers in droplet phase for differential sequence pairs at absolute T*=0.6 (A) Δκ=0.86 (sequence κ=1.0 and 0.14) (B) Δκ=0.54 (sequence κ=0.77 and 0.23) (C) Δκ=0.30 (sequence κ=0.65 and 0.35). Different mixing fractions has been shown in each panel ranging from $x_{Low-\kappa}$=0.1 to 0.9 with blue to green.

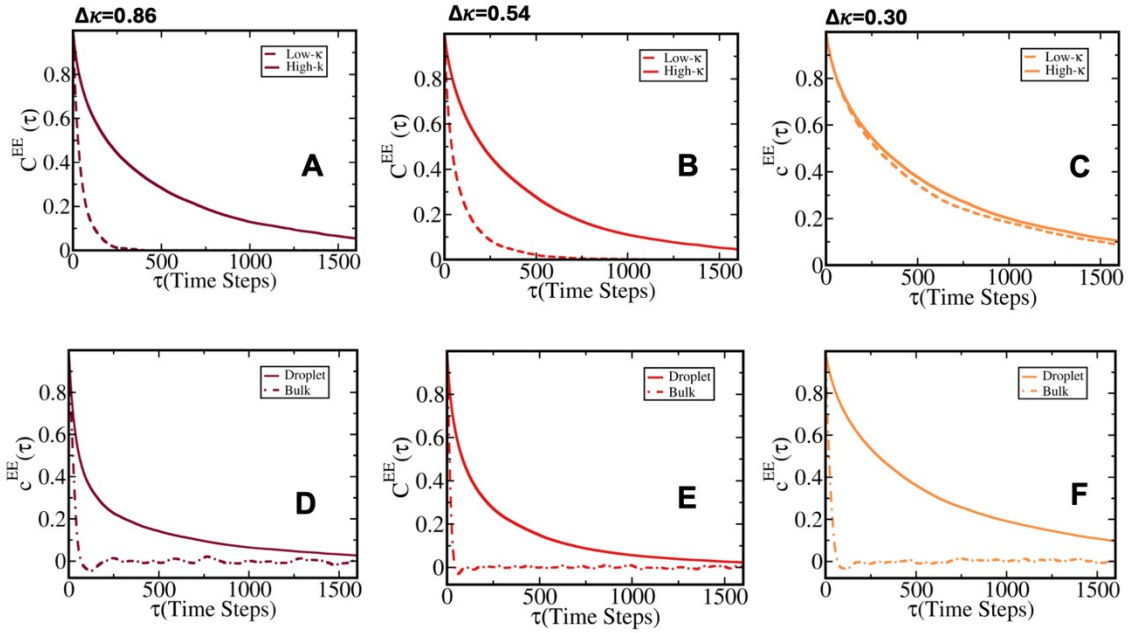

Figure S5: Chain reconfiguration time correlation analysis in droplet and bulk phase. Representative time correlation of end-to-end distance vector for low-κ and high-κ polymers in condensates at T/Tc=0.4 and mixing ratio $x_{Low-\kappa} = 0.5$ with sequence pairs (A) Δκ=0.86 (sequence κ=1.0 and 0.14) (B) Δκ=0.54 (sequence κ=0.77 and 0.23) (C) Δκ=0.30 (sequence κ=0.65 and 0.35). While solid line represents correlation for high-κ polymers, dashed line represent low-κ polymers. Representative average time correlation of end-to-end distance vector for polymers in condensate and bulk at T/Tc=0.4 and mixing ratio $x_{Low-\kappa} = 0.5$ with sequence pairs (D) Δκ=0.86 (sequence κ=1.0 and 0.14) (E) Δκ=0.54 (sequence κ=0.77 and 0.23) (F) Δκ=0.30 (sequence κ=0.65 and 0.35). While solid line represents correlation in droplet polymers while dot-dashed line represent the same in bulk. Color scheme represent individual Δκ variants respectively.

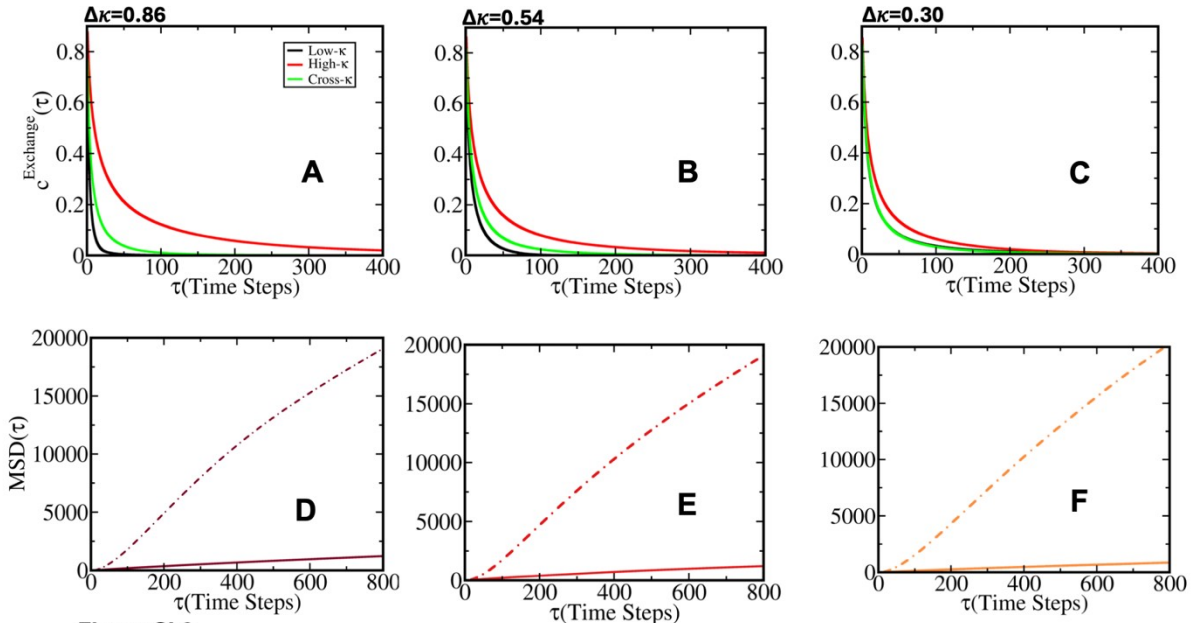

Figure S6: Representative time correlation of contact exchange in droplet phase among polymers at T/Tc=0.3 and $^{x_{Low-\kappa}=0.5}$ for sequence pairs (A) Δκ=0.86 (sequence κ=1.0 and 0.14) (B) Δκ=0.54 (sequence κ=0.77 and 0.23) (C) Δκ=0.30 (sequence κ=0.65 and 0.35). Each panel consists variants of contact lifetime correlation namely among polymers of low-κ (black), high-κ (red) and cross interaction among high and low κ polymers (green). A comparative analysis of average mean squared displacement (MSD) of polymers in droplet phase and bulk at T/Tc=0.3 and $^{x_{Low-\kappa}=0.5}$ for differential sequence pair condensates (A) Δκ=0.86 (sequence κ=1.0 and 0.14) (B) Δκ=0.54 (sequence κ=0.77 and 0.23) (C) Δκ=0.30 (sequence κ=0.65 and 0.35) at T=0. and $^{x_{Low-\kappa}=0.5}$ for sequence pairs.

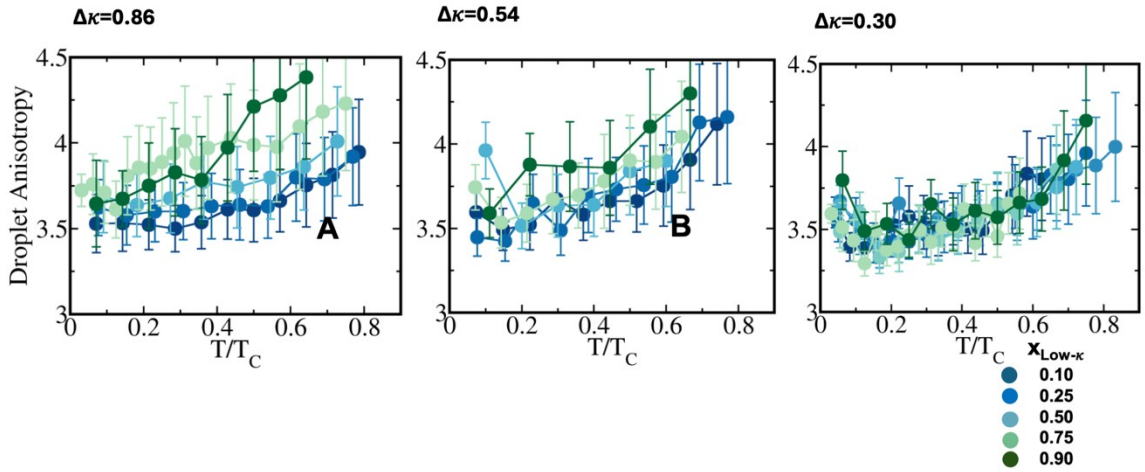

Figure S7: Shape anisotropy of droplets composed by differential sequence pairs along temperature scaled to criticality (A) Δκ=0.86 (sequence κ=1.0 and 0.14) (B) Δκ=0.54 (sequence κ=0.77 and 0.23) (C) Δκ=0.30 (sequence κ=0.65 and 0.35). Different mixing fractions has been shown in each panel ranging from $^{x_{Low-\kappa}}$=0.1 to 0.9 with blue to green.

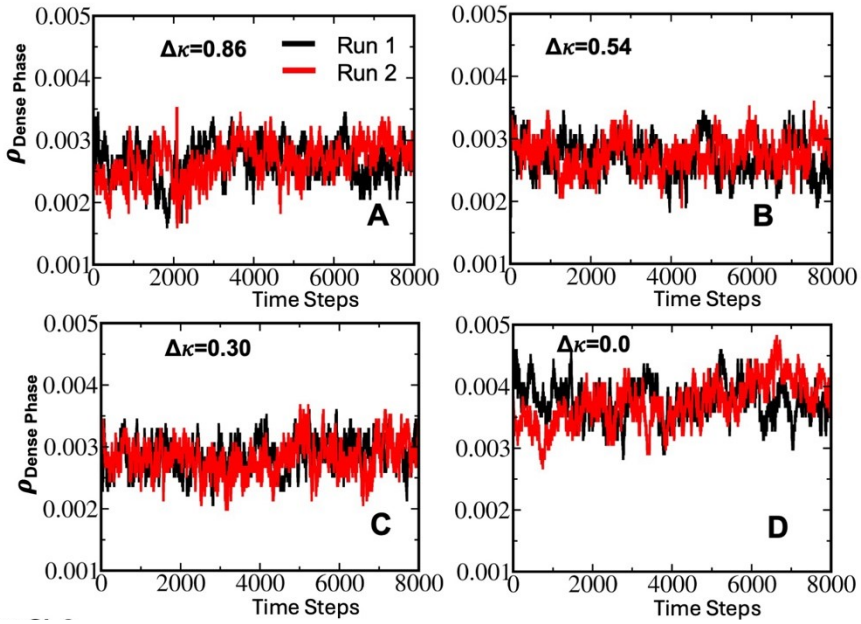

Figure S8: Convergence of droplet density. Density of largest cluster at $X_{Low\text{-}\kappa}$=0.5 and at T/Tc=0.4 for the studied systems (A) Δκ=0.86, (B) Δκ=0.54, (C) Δκ=0.30 and (D) Δκ=0.0 obtained from two independent runs as representative examples.

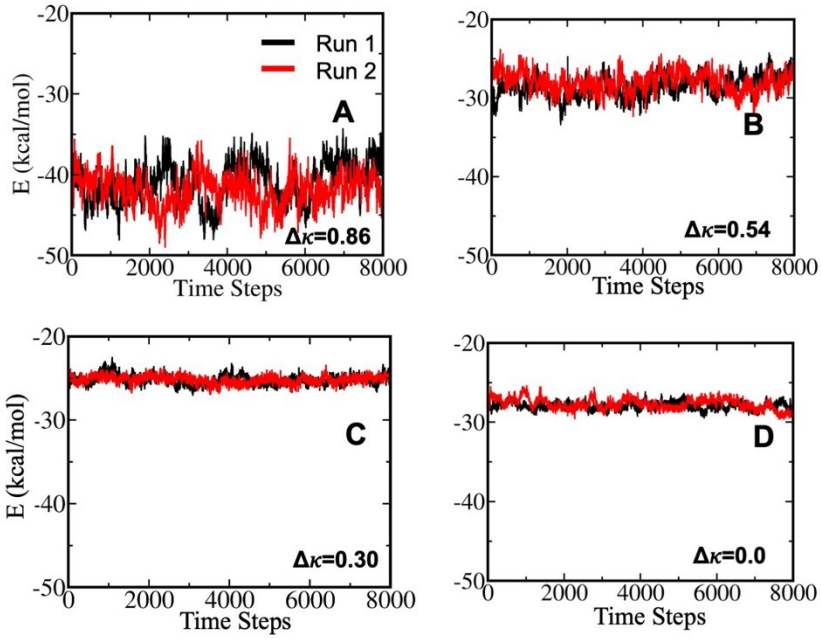

Figure S9: Convergence of electrostatic interaction energy in dense phase at $X_{Low\text{-}\kappa}$=0.5 and at T/Tc=0.4 for the studied systems (A) Δκ=0.86, (B) Δκ=0.54, (C) Δκ=0.30 and (D) Δκ=0.0 obtained from two independent runs as representative examples.

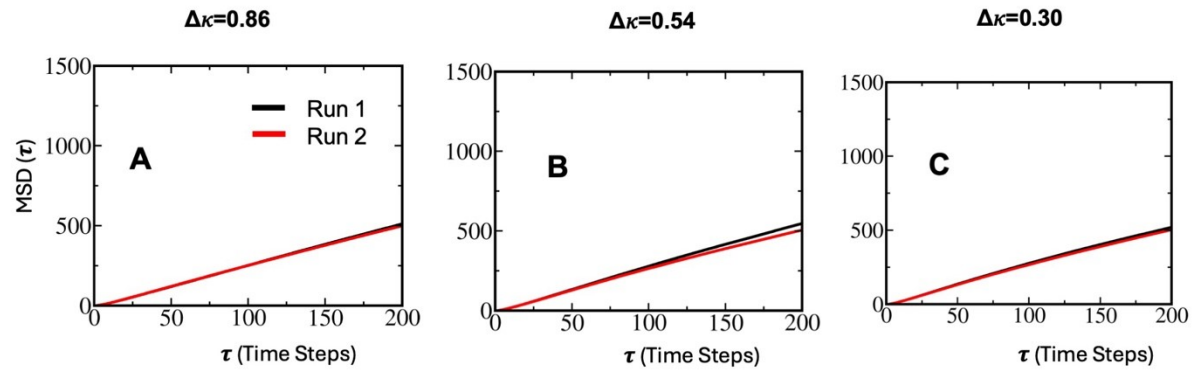

Figure S10: Convergence of mean squared displacements of high-κ polymers in droplet phase at $X_{Low\text{-}\kappa}$=0.5 and at T/Tc=0.4 for the studied systems obtained from two independent runs (A) Δκ=0.86, (B) Δκ=0.54, (C) Δκ=0.30 as representative examples.

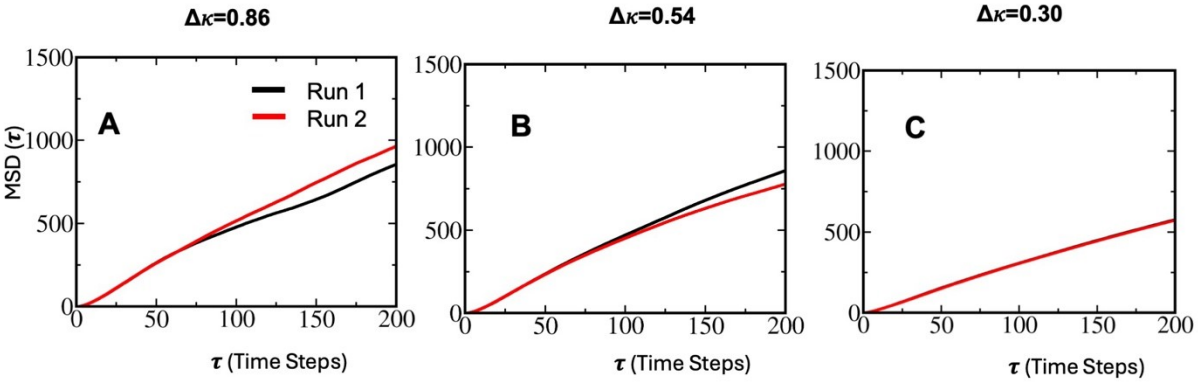

Figure S11: Convergence of mean squared displacements of low-κ polymers at $X_{Low\text{-}\kappa}$=0.5 and at T/Tc=0.4 for the studied systems (A) Δκ=0.86, (B) Δκ=0.54, (C) Δκ=0.30 obtained from two independent runs as representative examples.

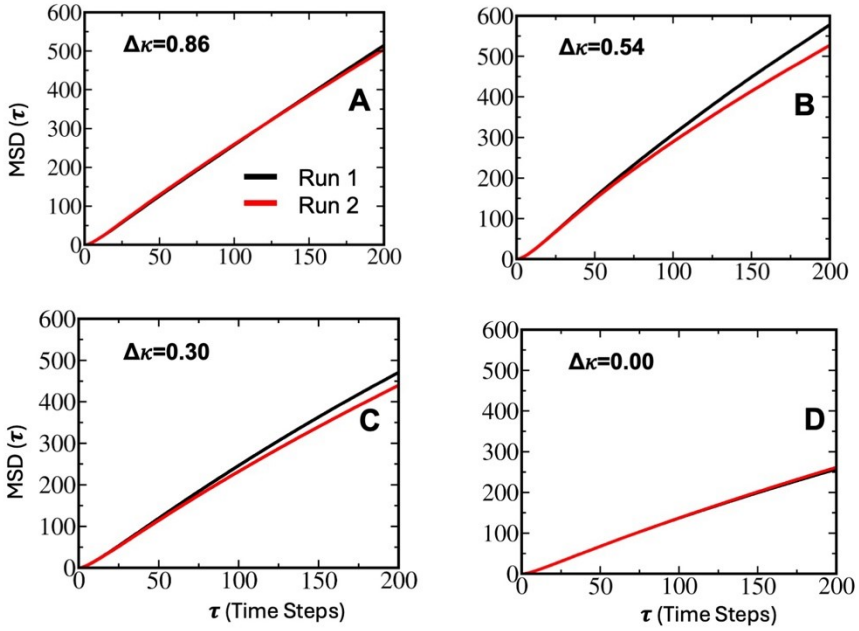

Figure S12: Convergence of average mean squared displacement of all polymers at $X_{Low\text{-}\kappa}$=0.5 and at T/Tc=0.4 for the studied systems obtained from two independent runs (A) Δκ=0.86, (B) Δκ=0.54, (C) Δκ=0.30 and (D) Δκ=0.0 as representative examples.

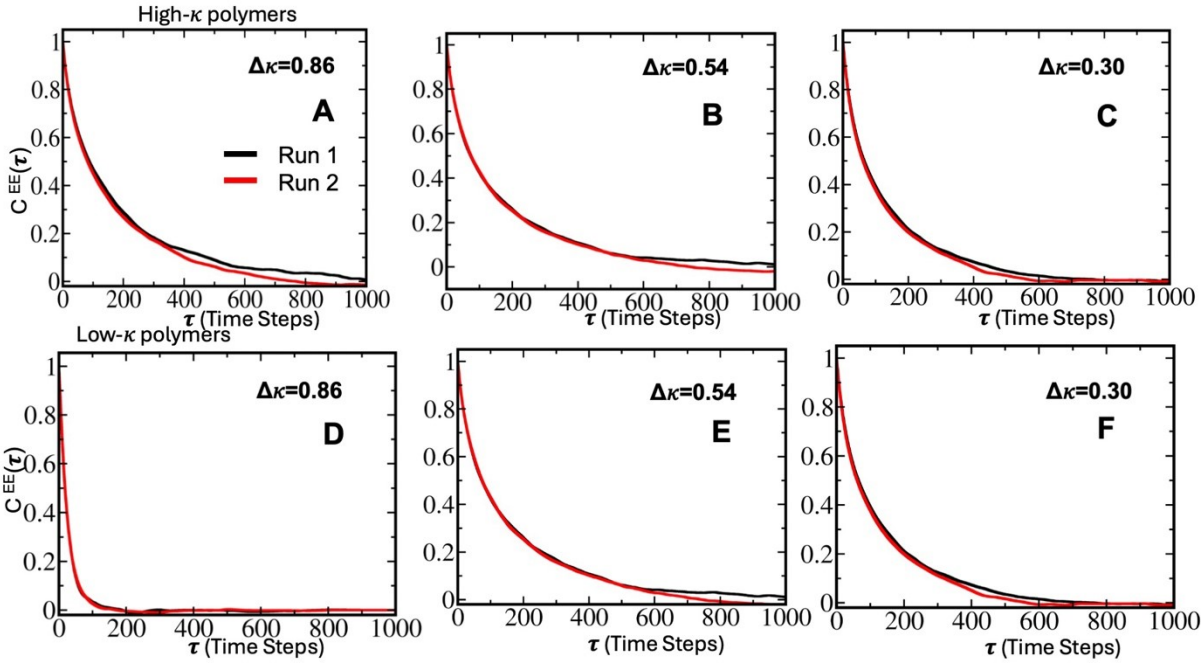

Figure S13: (A-C) Convergence of end-to-end distance time correlation function of high-κ polymers in droplet phase at $X_{Low\text{-}\kappa}$=0.5 and at T/Tc=0.4 for the studied systems obtained from two independent runs (A) Δκ=0.86, (B) Δκ=0.54, (C) Δκ=0.30 as representative examples. (D-F) Convergence of end-to-end distance time correlation function of low-κ polymers in droplet phase at $X_{Low\text{-}\kappa}$=0.5 and at T/Tc=0.4 for the studied systems obtained

from two independent runs (D) Δκ=0.86, (E) Δκ=0.54, (F) Δκ=0.30 as representative examples.

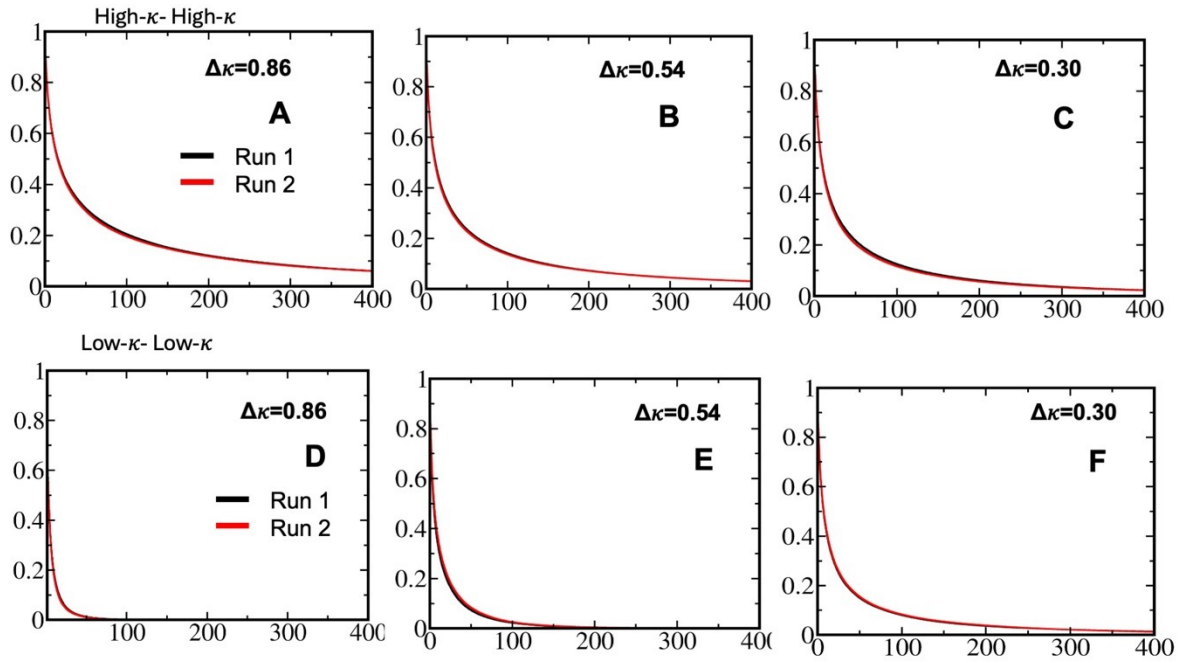

Figure S14: (A-C) Convergence of time correlation function delineating neighbour exchange kinetics of high-κ polymers in droplet phase at $X_{Low-\kappa}$=0.5 and at T/Tc=0.4 for the studied systems obtained from two independent runs (A) Δκ=0.86, (B) Δκ=0.54, (C) Δκ=0.30 as representative examples. (D-F) Convergence of time correlation function delineating neighbour exchange kinetics of low-κ polymers in droplet phase at $X_{Low-\kappa}$=0.5 and at T/Tc=0.4 for the studied systems obtained from two independent runs (D) Δκ=0.86, (E) Δκ=0.54, (F) Δκ=0.30 and as representative examples.

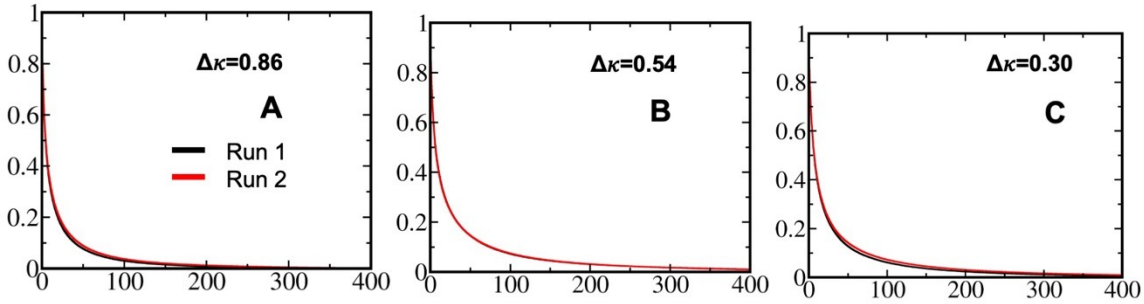

Figure S15: Convergence of time correlation function delineating neighbour exchange kinetics among high-κ and low-κ polymers in droplet phase at $X_{Low-\kappa}$=0.5 and at T/Tc=0.4 for the

studied systems obtained from two independent runs (A) Δκ=0.86, (B) Δκ=0.54, (C) Δκ=0.30 as representative examples.

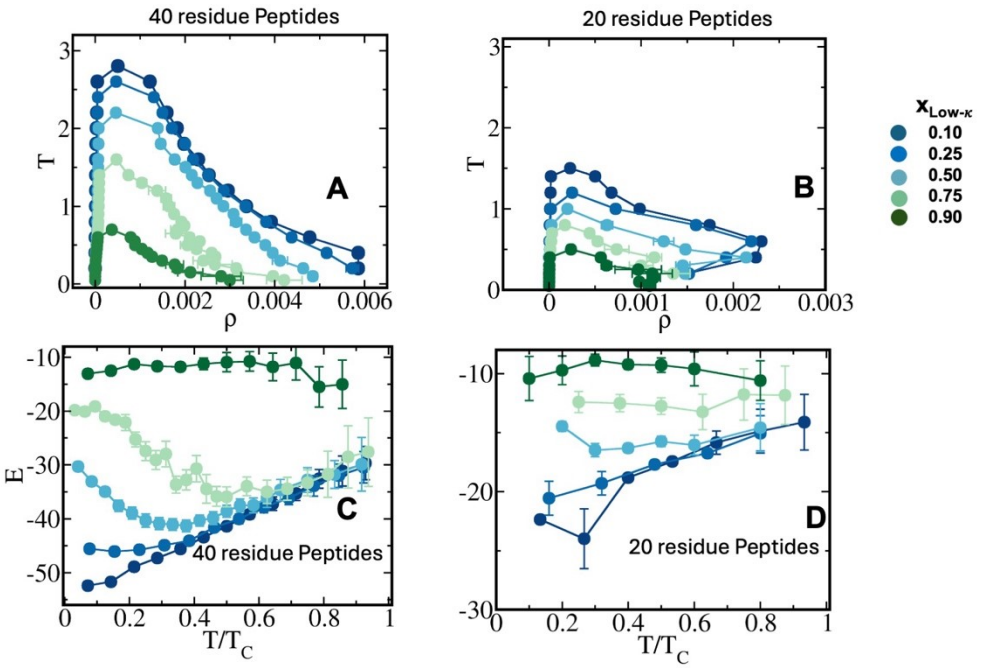

Figure S16: Phase diagrams for (A) 40-residue sequence pairs for Δκ=0.86 has been compared with their (B) 20-residue counterpart to elucidate finite size effect on the reported trends along mixing fractions. Similarly, energetics of droplets assembly has been shown for (C) Δκ=0.86 sequence pairs with 40-residues and (D) their 20-residue counterpart showcasing similar trends.

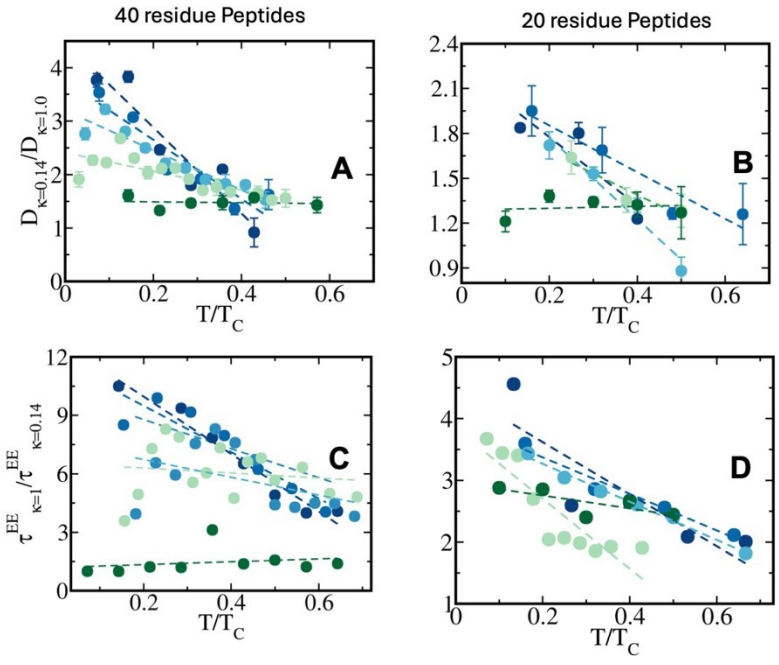

Figure S17: Effect of finite size on dynamics. Ratio of diffusivity between low-κ and high-κ ($\frac{D_{Low-k}}{D_{High-k}}$) polymers in condensate phase along temperature for Δκ=0.86 variant has been compared for systems with (A) 40-residue peptides (B) 20-residue peptides. Average chain reconfiguration lifetime compared among low-κ and high-κ ($\frac{\tau^{EE}_{high-k}}{\tau^{EE}_{Low-k}}$) polymers in condensate phase along temperature scaled to criticality for sequence pairs Δκ=0.86 having (A) 40-residue chains and (B) 20-residue chains.

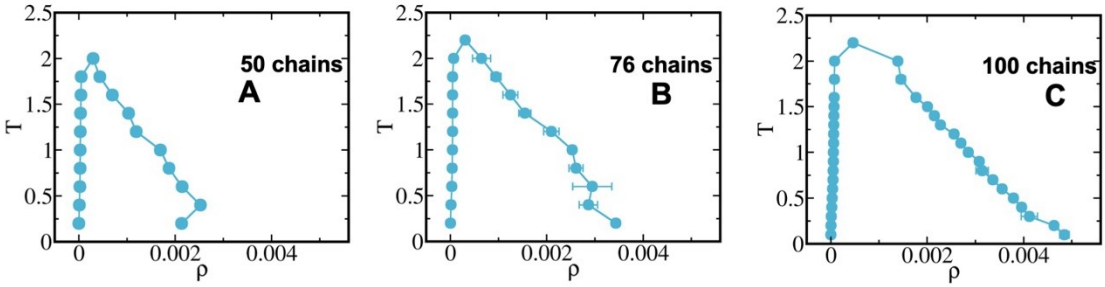

Figure S18: Representative convergence of phase diagrams obtained from different system sizes simulated for Δκ=0.86 variant at $X_{Low-\kappa}$ =0.5(A) 50 chains (B) 76 chains and (C) 100 chains in the same box $300 \times 300 \times 300$ Angstrom^3. The same critical points have been observed for all three systems simulated.